On the possibility to determine the gluon structure function in the ATLAS experiment using the direct photon away-side jet cross section at the LHC collider

El M. Abouelouafa, R. Cherkaoui
Laboratoire de Physique Nucléaire, Université de Rabat

ATL-PHYS-2001-014
27/09/2001

Abstract

In lowest order perturbative quantum chromodynamics, high transverse momentum direct photon production accompanied by a recoil hadronic jet is studied in LHC pp collisions at $\sqrt{s} = 14$ TeV. The gluon structure function for the proton in the range $0.005 < x < 0.04$ for Q^2 values between 440 GeV^2 and $2{\cdot}10^4$ GeV^2 is constrained assuming that the QCD Compton process gives the dominant contribution to high-p_T direct photon plus jet production.

1 Introduction

The production of high-p_T direct (prompt) photons in hadron collisions offers an important test of perturbative QCD. At leading order, we will show that this production is sensitive to gluons and thereby provides information on the gluon structure function for the proton.

In the present paper, the gluon structure function can be determined in the range $0.005 < x < 0.04$ and $440 < Q^2 < 2{\cdot}10^4$ GeV^2 (Sec. 6.2), by using the differencial cross section for the production of a direct photon and a opposite-side jet in LHC pp collisions at $\sqrt{s} = 14$ TeV. For this purpose we study the reaction $pp \longrightarrow \gamma$ + jet + X (where X are the undected hadrons), generated by the Monte Carlo PYTHIA (by which we modeled 100.000 events of the photon-jet type containing direct photons with high-p_T), and using the ATLFAST program to simulate the ATLAS detector at low luminosity ($10^{33}\ s^{-1}\ cm^{-2}$).

The simulation programs used for this analysis are briefly described in Sec. 2. The trigger and the selection criteria for photons and jets are given in Sec. 3. A description of direct photon production is discussed in Sec. 4, while Sec. 5 presents the cross section results for γ-jet simulated events. The method used to extract the gluon structure function and the main results are formulated in Sec. 6. The theoretical systematic errors are given in Sec. 7, followed by a conclusion in Sec. 8.

2 Simulation

2.1 The Lund Monte Carlo (MC)

The versions 5.7 of PYTHIA and 7.4 of JetSet [1] have been used to generate the γ-jet events in this paper. The Lund MC program is able to simulate pp interactions at $\sqrt{s} = 14$ TeV, corresponding to the nominal LHC energy. However, this program is limited to leading order (LO) processes (the basic processes are $2 \longrightarrow 2$ with the LO order matrix elements). A phenomenological model is introduced to describe the hadronisation of a final parton configuration.

2.2 ATLFAST

The γ-jet events which are generated with PYTHIA pass through an ATLFAST simulation of the detector. ATLFAST is a fast simulation program for ATLAS that is used for determining the performance of the detector for physics channels. This program is interfaced to the event generator. The stable final-state particles are processed and the reconstructed isolated momenta are smeared by gaussian resolution distributions to simulate the response of the ATLAS calorimeters. A complete description of ATLFAST is given in ref. [2].

3 Selection criteria and trigger

3.1 Selection criteria

The selection criteria are used to detect photons and jets. The photons are selected within the central part of the calorimeter and over the default energy nominal threshold:

$$|\eta(\gamma)| \ < \ 0.7, \ the\, default\, threshold\ (\ [2])\ \ p_T(\gamma) \ > \ 5\, GeV,$$

where $\eta(\gamma)$ and $p_T(\gamma)$ are the photon rapidity and the transverse momentum respectively. The selected photons are then passed through isolation criteria [2]. Similarly, pseudo-rapidity and transverse momentum requirements are imposed on the jets:

$$|\eta(jet)| \ < \ 2, \ p_T(jet) \ > \ 35\, GeV.$$

3.2 Trigger cuts

In this analysis, only the level 1 trigger is taken into account to select the high p_T events. However, the following cuts are assumed:

- minimum p_T for isolated photons, to discriminate the background, is 40 GeV (the selection of the ATLAS trigger at low luminosity) with a rapidity coverage $|\eta(\gamma)| < 0.7$.
- minimum jet transverse momentum is 37 GeV. The rapidity coverage for jets is $|\eta(jet)| < 2$.

4 Direct photons and QCD

In quantum chromodynamics (QCD) the two hard processes that contributes to direct photons production at lowest order in the strong runing coupling constant $\alpha_s(Q^2)$ are the

Compton effect on gluons $gq \longrightarrow \gamma q$ and the annihilation $q\overline{q} \longrightarrow \gamma g$. The cross section expressions at the parton level for these two elementary processes after performing spin average and color sums are respectively [3]:

$$\frac{d\sigma}{d\hat{t}}(gq) = -\frac{\pi\alpha\alpha_s}{\hat{s}^2}\cdot\frac{e_q^2}{3}[\frac{\hat{u}}{\hat{s}} + \frac{\hat{s}}{\hat{u}}] \qquad (1)$$

$$\frac{d\sigma}{d\hat{t}}(q\overline{q}) = -\frac{\pi\alpha\alpha_s}{\hat{s}^2}\cdot\frac{8e_q^2}{9}[\frac{\hat{u}}{\hat{t}} + \frac{\hat{t}}{\hat{u}}] \qquad (2)$$

where $\hat{s}$,$\hat{t}$ and $\hat{u}$ are the Mandelstam variables for the parton-parton scattering processes and e_q is the fractional charge of the qth quark.

In the parton model, neglecting the internal transverse motion of partons k_T, the differential cross section at LO for the process $A+B \longrightarrow \gamma+jet+X$ in the center of mass is given by [4]:

$$\frac{d^3\sigma(AB \longrightarrow \gamma + jet + X)}{dp_T d\eta_\gamma d\eta_{jet}} = 2p_T \sum_{ab} x_a x_b F_a^A(x_a, Q^2) F_b^B(x_b, Q^2) \frac{d\sigma(ab \longrightarrow \gamma + jet)}{d\hat{t}} \qquad (3)$$

where x_a and x_b are defined to be the momentum fractions for the hadrons A and B respectively and p_T is the photon transverse momentum. From the photon and jet rapidities η_γ and η_{jet} and with $x_T = 2p_T/\sqrt{s}$, the momentum fractions x_a and x_b at LO are given by:

$$x_a = \frac{x_T}{2}(e^{\eta_\gamma} + e^{\eta_{jet}}) \; and \; x_b = \frac{x_T}{2}(e^{-\eta_\gamma} + e^{-\eta_{jet}})$$

Note that for the case of direct photon production plus opposite-side jet, x_a and x_b can be approximated at next-to-leading order by the expressions above (i.e. higher order corrections introduce a small contribution [5]). $F_a^A(x_a, Q^2)$ and $F_b^B(x_b, Q^2)$ are the parton distribution functions. In the approximation where the contribution of the annihilation process is neglected (see fig. 1), the cross section for producting a jet opposite to a direct photon in pp collisions (eq. (3)) becomes:

$$\frac{d^3\sigma}{dp_T d\eta_\gamma d\eta_{jet}} = \frac{2\pi p_T \alpha\alpha_s}{3\hat{s}^2}[F_2(x_a, Q^2) x_b G(x_b, Q^2)\frac{\hat{s}^2 + \hat{t}^2}{-\hat{s}\hat{t}} + F_2(x_b, Q^2) x_a G(x_a, Q^2)\frac{\hat{s}^2 + \hat{u}^2}{-\hat{s}\hat{u}}] \qquad (4)$$

In this expression $G(x, Q^2)$ is the gluon structure function. In the quark parton model the structure function $F_2(x, Q^2)$ is given by

$$F_2(x, Q^2) = \sum_f e_f^2 x F_f(x, Q^2) \quad (with \; f = 1, \cdots, N_f; \; N_f \; is \; the \; number \; of \; flavours)$$

where e_f is the charge of the quark of flavour f which has a momentum distribution $F_f(x, Q^2)$.

5 Results of cross section for γ-jet simulated events

In order to regularize the differential cross section divergence at $p_T \longrightarrow 0$, the QCD processes for direct photon production are generated with a transverse momentum greater than 37 GeV (the threshold on the jet p_T). The γ-jet sample is then selected by requiring an additional analysis cut: the azimuthal separation between the photon and the jet directions must satisfy: $150^\circ < \triangle\phi_{\gamma-jet} < 210^\circ$. Notice that the π° and η particles

(the only particles which survive to isolation criteria with a small rate[1]) are forced to be stable (in the first approach) and the Bremsstrahlung from quarks (initial and final-state radiation corrections[2]) are taken into account in the study presented in this paper. For the following studies in this section, the CTEQ4L [7] set has been used to parametrize the proton structure function. To calculate the observed cross section from ATLFAST, we adopted the following formula:

$$\sigma_{ATLFAST} = \frac{Number\ of\ accepted\ events}{Number\ of\ generated\ events} \cdot \sigma_{PYTHIA},$$

where σ_{PYTHIA} is the cross section from PYTHIA. The results for the double inclusive cross section for the production of direct photons and recoil jets with this additional cut are shown in fig. 1, as a function of the photon transverse momentum, for an integrated luminosity of 100 pb^{-1}.

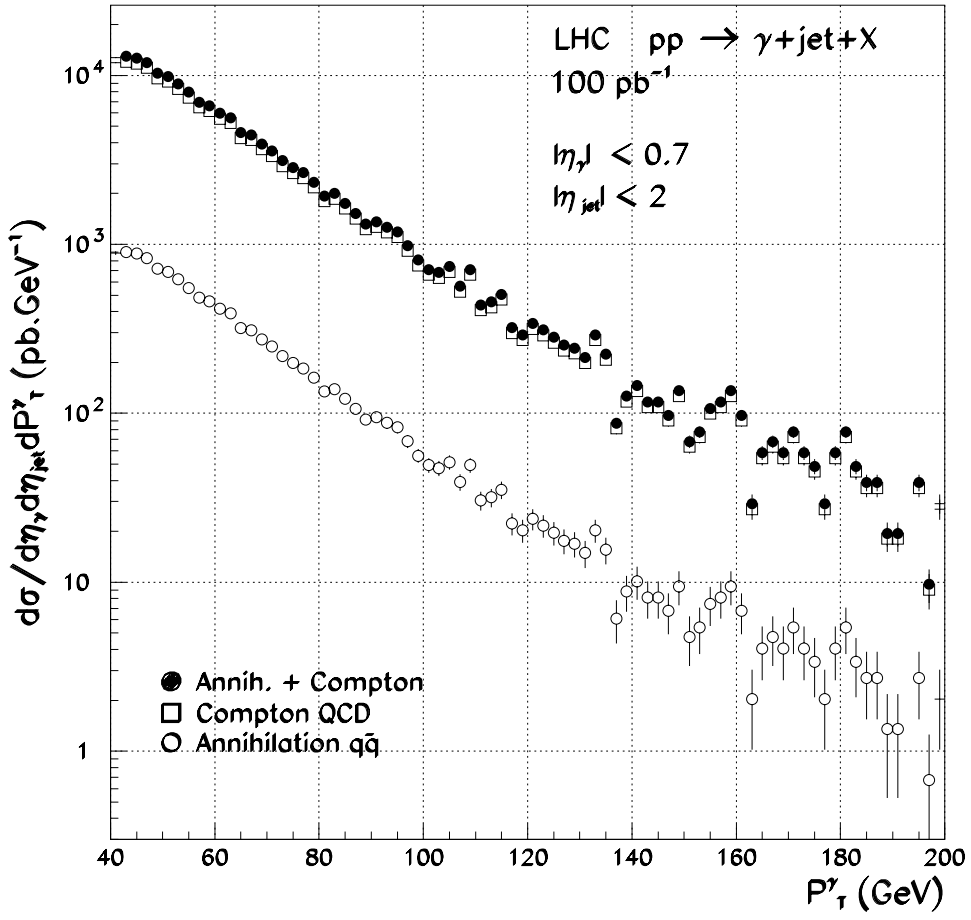

Figure 1: Direct-photon production with an opposite-side jet in pp collisions at $\sqrt{s} = 14$ TeV and the CTEQ4L structure functions, as a function of p_T^γ

[1]In the study of a large scale jet production shows that only 28% of the photons at high p_T from π° decays survive to isolation criteria, compared to 84% of the direct and bremsstrahlung samples [6].

[2]The bremsstrahlung sample is generated by switching on the photon emission in the Pythia MC program [1].

The assumed luminosity of 100 pb^{-1} corresponds to about one day of data taking with low luminosity. The dominance of the Compton process $qg \longrightarrow q\gamma$ over the annihilation $q\overline{q} \longrightarrow g\gamma$ is clearly illustrated in fig. 1. In γ-jet production, the contribution of the annihilation channel to the cross section is less than 10 %. A relatively pure quark-jet sample in $pp \longrightarrow \gamma + jet$ events has been studied. In this study, the same p_T cuts of Sec. 3 are used whereas the η range of the photons and jets are restricted to $|\eta| < 2.5$ and $|\eta| < 3.2$, respectively. The fraction of these events correponding to the quarks (u, d, s, c and b) for Compton and annihilation processes in the total $\gamma - jet$ sample is plotted in fig. 2 as a function of the photon pseudo-rapidity ($|\eta(\gamma)| < 2.5$) and an integrated luminosity of 100 pb^{-1}. Up-quark jets clearly dominate (because of the quark structure of the proton), while the contribution of bottom-quark jets in the total $\gamma - jet$ sample is very small.

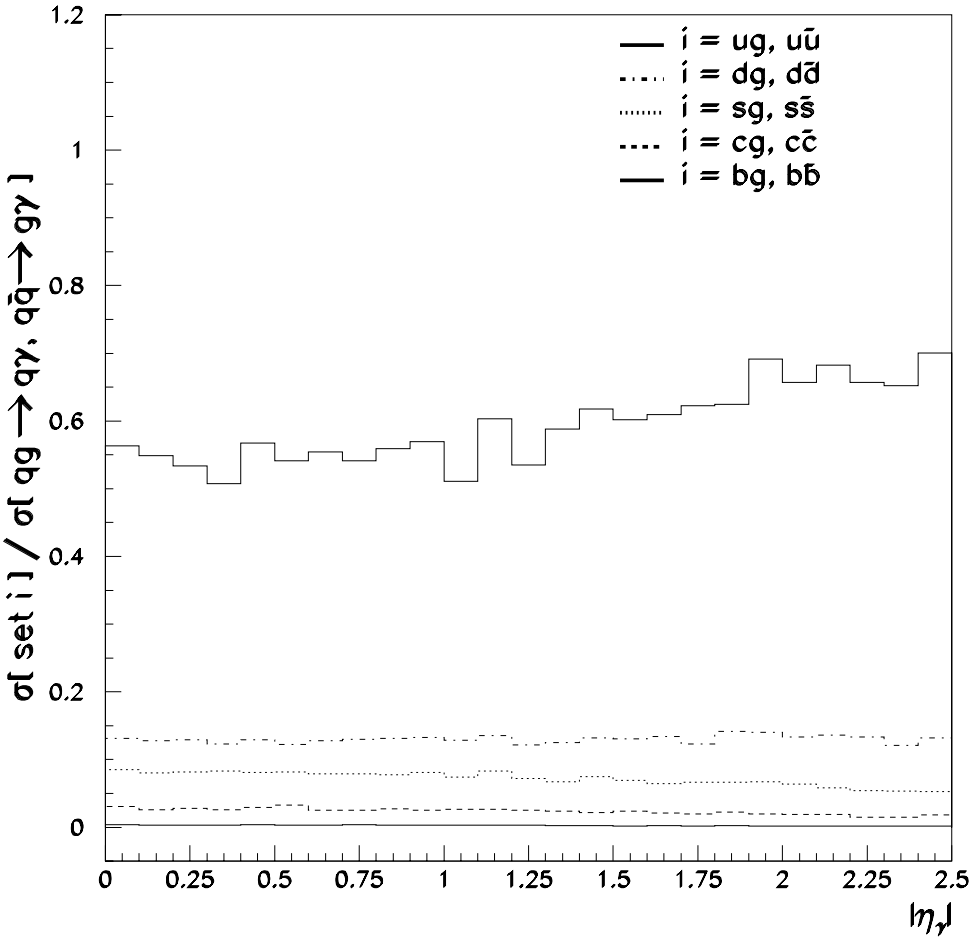

Figure 2: Fraction of $pp \longrightarrow \gamma + jet$ events for u, d, s, c and b-quark channels (see text)

The effect on the cross section of using different structure functions has been tested for three sets of parton distributions, CTEQ4HJ [7], MRS(A) [8] and GRV94HO [9]. The relative difference of the cross section between these sets of parton distributions and the CTEQ4L parametrization is shown in fig. 3 as a function of the photon pseudo-rapidity

(with $|\eta(\gamma)| < 2.5$). The rapidity range for jets is restricted to $|\eta| < 3.2$. The variation obtained is less than 10 %.

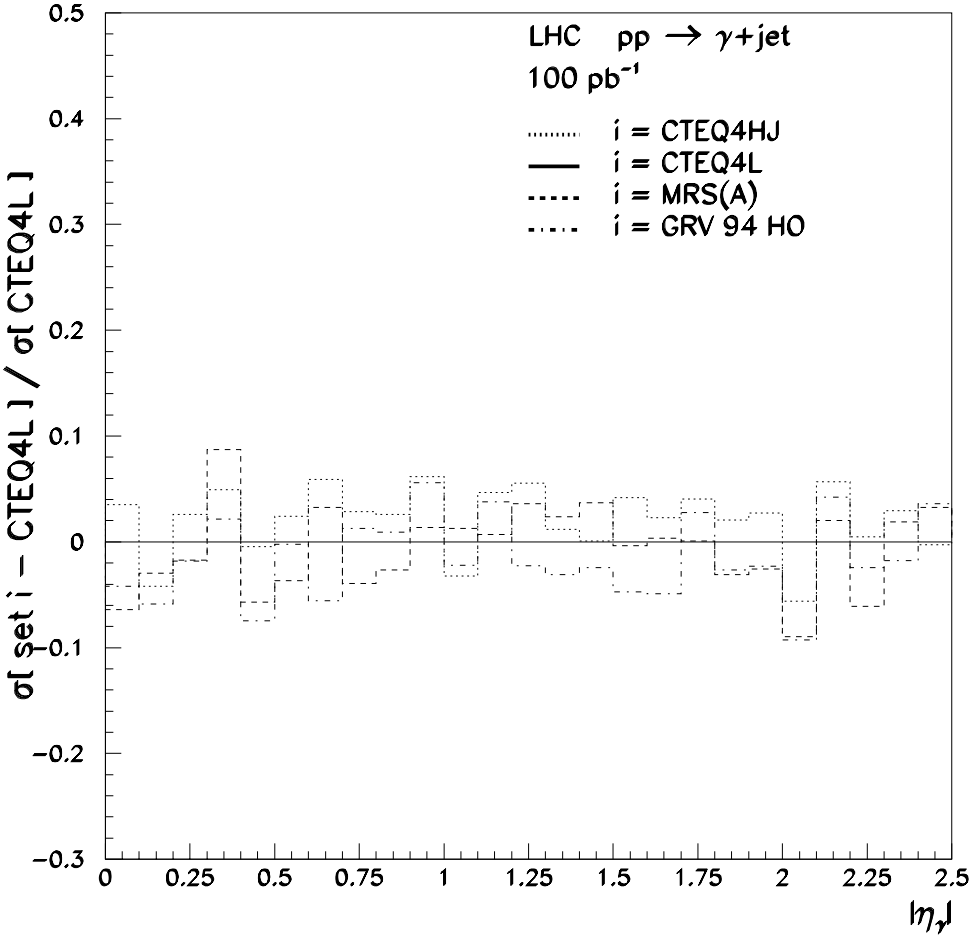

Figure 3: Cross section ratios from ATLFAST of the $\gamma - jet$ production between structure functions. CTEQ4L is taken as reference system.

Notice that the pseudo-rapidity distribution of the photon shows a flat behaviour in the central part of the detector (fig. 2). This will favor the photon rapidity requirement discussed in Sec. 3, in order to study the gluon strcture function, while the cutoff on the jet direction is purely kinematical.

6 Determination of the gluon structure function

6.1 Method

The method used to extract the gluon structure function is based on fitting the $\gamma - jet$ cross section to the theoretical prediction at leading order. The data are simulated by using the Martin-Roberts-Stirling set A [MRS(A)] structure function set [8] in the program Pythia, as a reference system (according to the choice of the parametrization for $F_2(x, Q^2)$,

as will be described later). The eq. (4) defined in Sec. 4 has been used for this purpose. In this expression it is assumed that the dominant hard process contributing to direct photon production is the Compton effect on the gluon. $F_2(x,Q^2)$ is expressed in terms of singlet and non-singlet parts via [10]

$$F_2(x,Q^2) = \frac{5}{18}F_2^S(x,Q^2) + \frac{1}{6}F_2^{NS}(x,Q^2)$$

The MRS(A) set is used to parametrize the structure function F_2 from ref. [11] (in the analysis of deep inelastic scattering "DIS", in particular, the measurements of F_2^p at HERA, shows that this set of quark distribution functions is consistent with the data obtained). The strong coupling constant is given at the next-to-leading order by

$$\alpha_s(Q^2) = \frac{1}{b\ ln(Q^2/\Lambda^2_{\overline{MS}})}[1 - \frac{b'\ lnln(Q^2/\Lambda^2_{\overline{MS}})}{b\ ln(Q^2/\Lambda^2_{\overline{MS}})}] \qquad (5)$$

with the $\Lambda_{\overline{MS}}$ value being chosen according to the parton distribution function parametrization and

$$b = \frac{11C_A - 2N_f}{12\pi}\ ,\ b' = \frac{17C_A^2 - 5C_AN_f - 3C_FN_f}{2\pi(11C_A - 2N_f)}$$

where $C_A = N_c$ (number of colors) and $C_F = N_c^2 - 1/2N_c$ for SU(N_c).

The scale which enters in the structure functions and α_s is chosen to be the same, $Q^2 = p_T^2/4$ (according to the appropriate choice of the scale for α_s from ref. [12]). The Q^2 dependence of the gluon distribution (values) is neglected in our analysis. The error induced is estimated less than 10% (Sec. 6.2). Thus, the gluon structure function is taken to have the generic form [13]

$$xG(x) = A_0x^{A_1}(1-x)^{A_2}\cdot P(x;A_3,\cdots)$$

with $A_{1,2}$ being physically associated with small-x Regge behavior and large-x valence counting rules respectively. For the smooth function P, the CTEQ parametrization is adopted

$$P(x;A_3,A_4) = 1 + A_3x^{A_4}$$

6.2 Results

In this section, the gluon structure function $xG(x)$ has been determined in the range $0.005 < x < 0.04$ covered by our data simulation (in the kinematic region defined by the photon transverse momentum $p_T(\gamma) > 40$ GeV and the rapidity cuts of the photon and jet $|\eta_\gamma| < 0.7$ and $|\eta_{jet}| < 2$, respectively). Fig. 4 shows the kinematic region analysed in this paper.

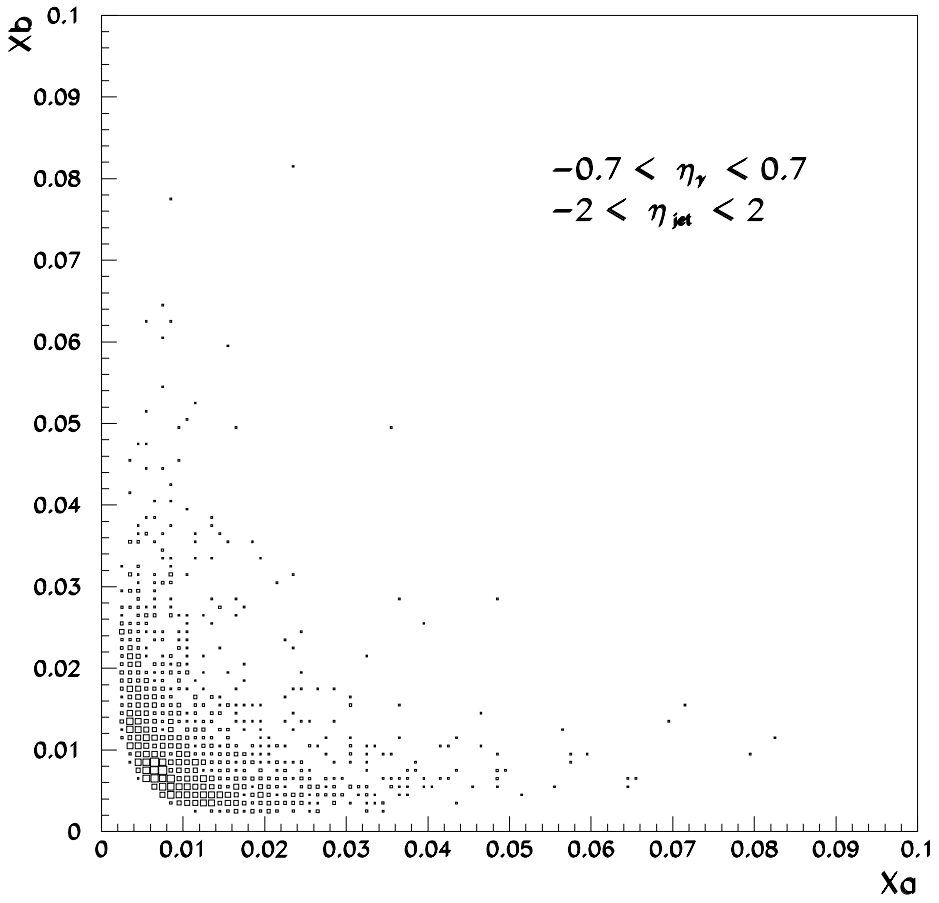

Figure 4: Two dimensional ($x_a \times x_b$) plot for event distributions from the reaction $pp \longrightarrow \gamma + jet + X$ at $\sqrt{s} = 14$ TeV and $p_T^\gamma > 40$ GeV.

In the previous section, it has been shown that the contribution of the b-quark jets is very small and can be neglected. In this case, the least-squares fits are made with four flavours of quarks. The fits are performed using the program MINUIT [14], taking into account the statistical and theoretical systematic errors. We notice that the systematic error is due to the choice of the parton distribution functions. This latter has been estimated in Sec. 4 as being less than 10 %. The χ^2 value is computed after adding the statistical and theoretical systematic errors in quadrature. The fact that this analysis is limited to the small-x region implies that the gluon distribution is mainly sensitive to the parameter A_1. In this regard, the parameter A_2 has been fixed to the value which

best describes the simulated data which is obtained for $A_2 = 3.0$ with $\chi^2 = 32.74/35$ DF (degree of freedom). Also, we introduced an effective K factor to take into account the contribution to the cross section for photon and recoil jet production from the pair annihilation process $q\overline{q}$ and the Bremsstrahlung effect from quarks (the main effect of the higher-order corrections). The results are given in table 1 for fits with the parameter K kept free. The main observation is that the χ^2 does not change as a function of K factor and the value of K is close to 1 because Pythia is LO. We also see that the K factor and the parameter A_0 are correlated and the errors are large if both are varied at once. In fig. 5 the result of the gluon structure function $xG(x)$ for an integrated luminosity of 10 fb^{-1}, as a function of x ($x_T = 2p_T/\sqrt{s}$), is compared to the HMRS B1 (with $\Lambda^{(4)}_{\overline{MS}}$=190 MeV) [15] theoretical parametrization. The errors on $xG(x)$ are statistical. In this case the average Q^2 is determined from the simulated data of the ATLAS experiment is $< Q^2 > = 576$ GeV^2. The agreement between the theoretical predictions and the simulated data is good, within the overall uncertainties (if we take also the theoretical systematic errors into account that will be discussed in the next section).

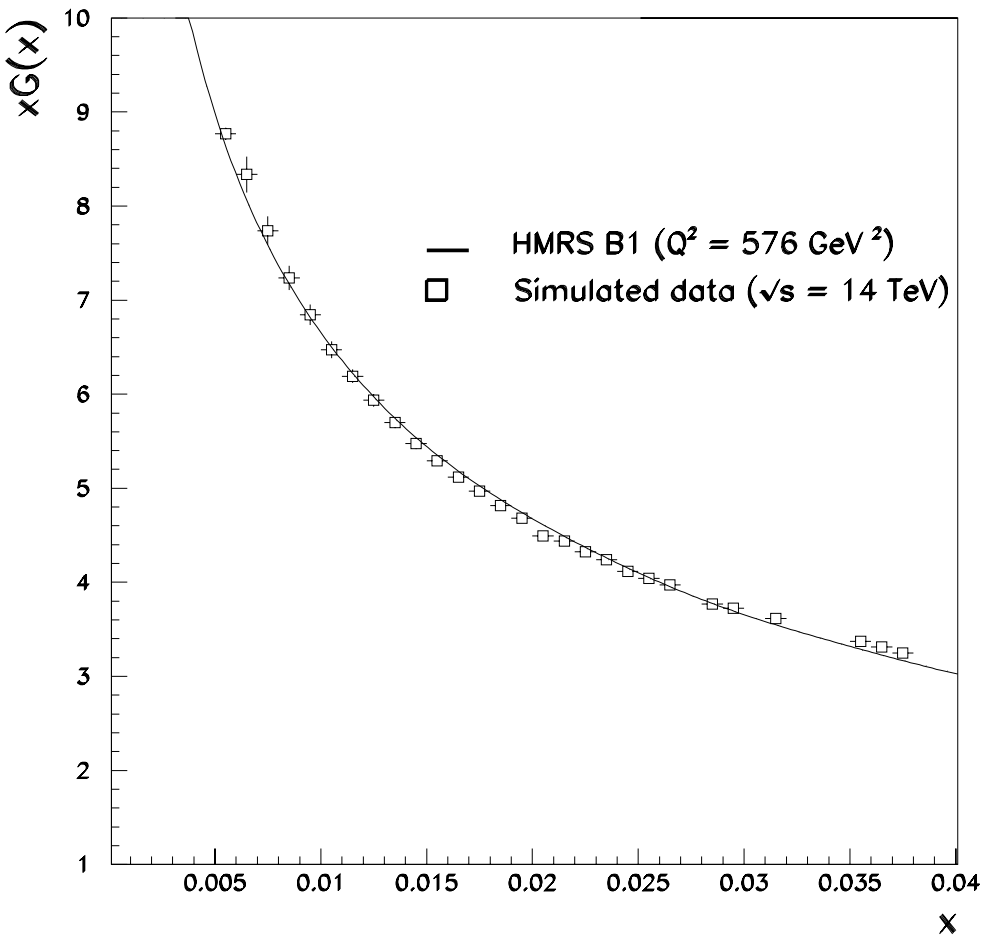

Figure 5: Comparison between the gluon structure function obtained from the simulated data using the MRS(A) structure functions and the parametrization HMRS B1

To evaluate the difference between theory and simulated data, the new sets of gluon distribution functions have been studied: MRST98-5 (with $\Lambda^{(4)}_{DIS}$=383 MeV) [16], MRS D0' (with $\Lambda^{(4)}_{\overline{MS}}$=230 MeV) [17], CTEQ 5D (with $\Lambda^{(4)}_{DIS}$=326 MeV) [18], ABFOW (with $\Lambda^{(4)}_{\overline{MS}}$=230 MeV) [19] and MTS1 (with $\Lambda^{(4)}_{\overline{MS}}$=212 MeV) [20]. In fig. 6 the relative difference of the gluon structure function between the unfolded simulated data and the theoretical predictions is shown as a function of x ($x_T = 2p_T/\sqrt{s}$). Clearly shown in this figure is that the variation is less than 5 % (reaching up to about 8% for CTEQ 5D) in the region $x < 0.03$. For $x \geq 0.03$ the variation is less than 5 % in the case of the HMRS B1 parametrization and it is within 5-8 % from the other sets, except CTEQ 5D where the variation is more than 10 %. There is much interest in comparing this result with the other input shapes of the gluon structure function. To do this, the following two generic forms have been studied by applying the method described in this paper:

- *MRS parametrization* ([13]) $\qquad xG(x) = A_0 x^{A_1}(1-x)^{A_2}\cdot(1 + A_3\sqrt{x} + A_4 x)$
- *DO parametrization* ([21]) $\qquad xG(x) = A_0 x^{A_1}(1-x)^{A_2}\cdot(1 + A_3 x + A_4 x^2)$

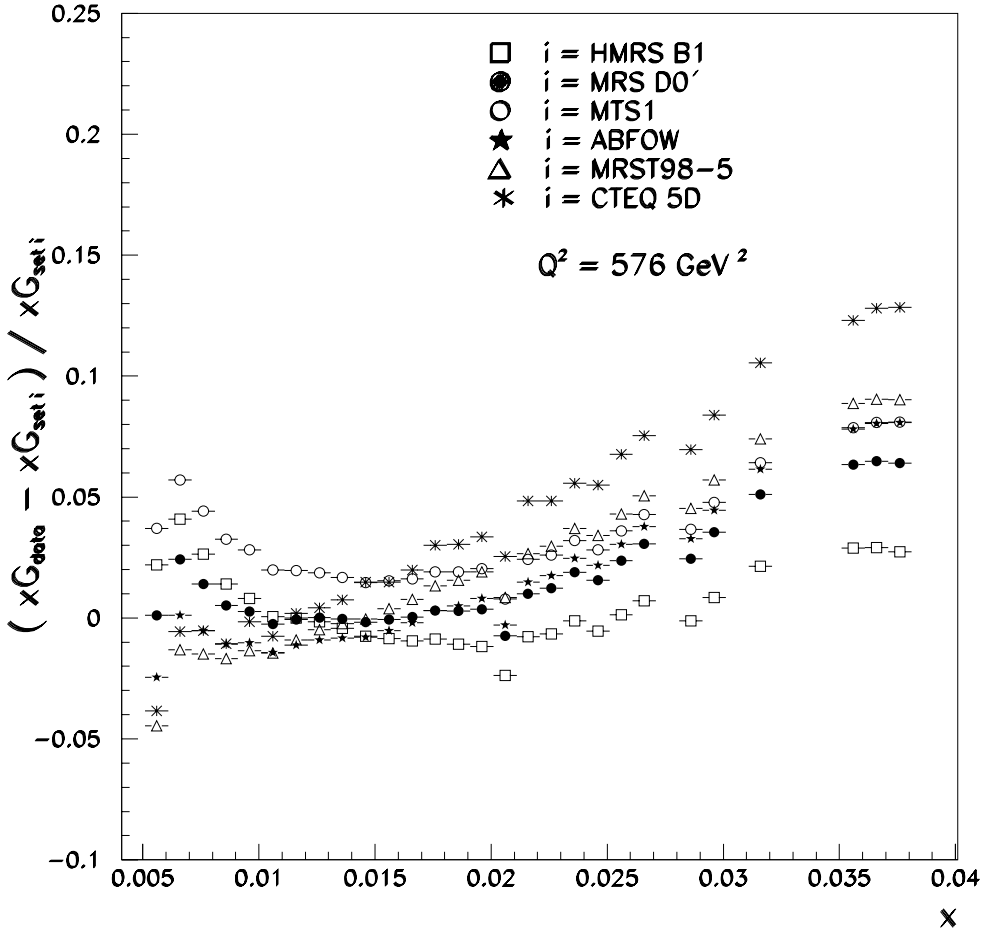

Figure 6: Gluon structure function ratios between the simulated data using the MRS(A) structure functions and the predictions at Q^2 = 576 GeV^2

Notice that the DO smooth function P given in ref. [21] is a polynom of degree 3. For each parametrization, the value of the χ^2 between the simulated data (using the MRS(A) structure functions) and the prediction is calculated. The results are summarized in table 1 and plotted in fig. 7. The χ^2 of the studied parametrizations shows a good agreement between theory and simulated data. Fig. 7 shows the comparison of the results on the gluon structure function to the CTEQ gluon input shape (which agree the best with the simulated data) for an integrated luminosity of 10 fb^{-1}. On this plot, the DO gluon input shape shows a consistency for $x < 0.02$ with respect to the "best" gluon distribution function. Whereas in the case of MRS gluon distribution function the agreement is noticeable for $x > 0.02$. Thus, the difference observed between the CTEQ and DO (CTEQ and MRS) gluon distribution functions varies from 7.5 to 20 % (8 to 15 %).

From table 1, we found, that the values of the A_1 parameter obtained agree well with the theoretical prediction of BFKL (Balitsky-Fadin-Kuraev-Lipatov dynamics) [11, 22]. The value of A_1 is given by the best fit : A_1=-0.51±0.18 .

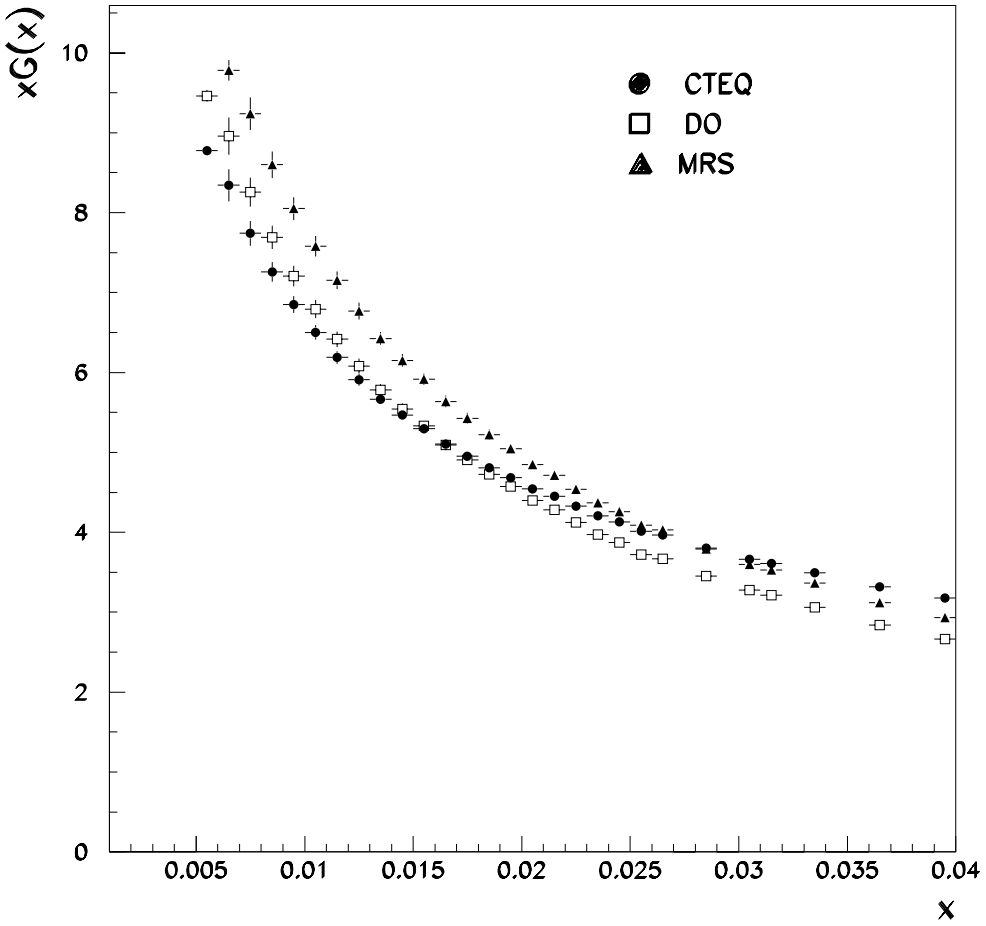

Figure 7: Results on the gluon structure function using different parametrizations of $xG(x)$ (see text)

parameters	gluon structure function shape		
	CTEQ	DO	MRS
K	0.96±0.85	1.16±0.94	1.00±0.86
A_0	0.65±0.58	0.81±0.65	2.18±1.88
A_1	-0.51±0.18	-0.49±0.18	-0.37±0.21
A_2	3.0	3.0	3.0
A_3	1.73±0.18	-7.56±0.79	-3.92±0.35
A_4	1.03±1.00	34.84±8.21	5.94±1.08
χ^2	32.74	37.02	37.23
DF	35	35	34

Table 1 : The results of fits obtained by using the MRS(A) set of quark distributions and $\mathbf{Q^2 = p_T^2/4}$

In addition, some correlation between the K factor and the gluon structure function is obtained (the fitted parameters A_i of $xG(x)$ show a correlation with the effective K factor).

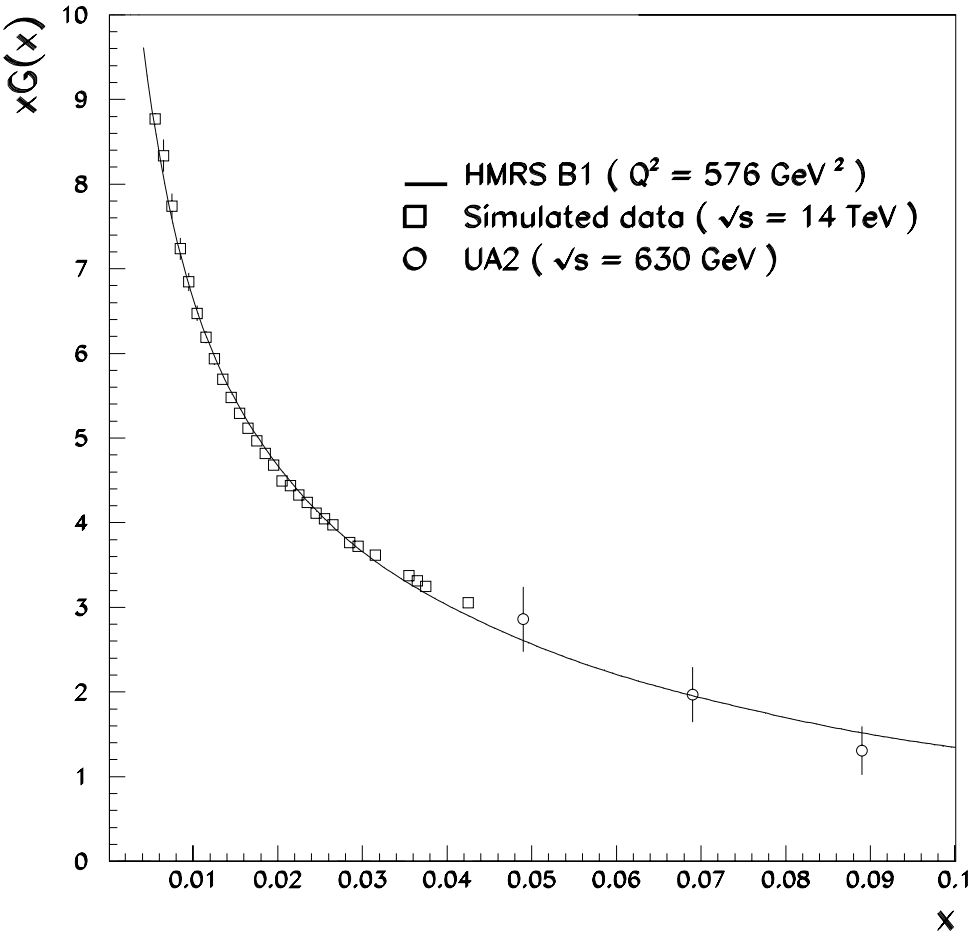

Figure 8: A comparison between theoretical predictions and the two data sets for gluon. The data are from our simulation of ATLAS detector (the errors on $xG(x)$ are statistical) and UA2 experiment

We end this analysis by comparing our result to the gluon structure function constrained by the UA2 data for $p\overline{p}$ collisions [23]. One should notice that the data points used correspond to the small-x values accessible by this experiment ($\sqrt{s}$ = 630 GeV). These data points are consistent with the theoretical gluon parametrization HMRS B1 at the Q^2 value given by our simulation (fig. 8), within the overall uncertainties (experimental and theoretical added in quadrature). This confirms the compatibility of our results and the good agreement with theory.

To conclude we emphasize that the minimum transverse momentum of the photon required in this study is at least 40 GeV. However, we have studied the effect on the gluon structure function by using for the transverse momentum cut: $p_T(\gamma) > 60$ GeV (threshold of the single photon trigger). The variation obtained (the difference between the gluon structure functions for the $p_T(\gamma)$ cuts of 40 GeV and 60 GeV, respectively) is less than 2 %.

7 Theoretical systematic errors

Owing to the weak dependence of the $\gamma - jet$ cross section on the QCD energy scale Λ_{QCD}, this latter cannot be obtained from our simulation. The systematic uncertainty due to the choice of $\Lambda^{(4)}_{\overline{MS}}$ is evaluated by changing the value of $\Lambda^{(4)}_{\overline{MS}}$ in α_s (Eq. (5)) in the range from 155 to 395 MeV (for $Q = p_T/2$). Therefore, the variation on $xG(x)$ is from 5 to 6 %.

The effect of the uncertainty on $xG(x)$ due to the ambiguity in the Q^2 choice has been studied by using the following representations of the p_T dependence: $Q^2 = p_T^2/9$, $Q^2 = p_T^2/4$ and $Q^2 = p_T^2$. The systematic error obtained is less than 5 %.

In the previous section, the error resulting from the difference between the studied gluon input shapes DO and MRS to the one of CTEQ gives an uncertainty within 7.5-20%.

In order to estimate the error due to the choice of the quark distribution functions, we have repeated the fit procedure above by using the CTEQ4L set to parametrize $F_2(x, Q^2)$ in eq. (4). Here, the CTEQ4L set is used as a parametrization of the proton stucture function in the MC program. Hence, the error on $xG(x)$ evaluated in this way is found to be about ± 3 %. Combining quadratically these uncertainties, the total theoretical error is estimated to be about 11.2-21.7 %. Such an error is induced by using the cross section at LO which, generally, have large estimated errors. An obvious way to improve upon this (theoretical uncertainty dominating the measurement) is to use the next-to-leading order cross sections.

8 Conclusion

Throughout this paper, we have presented a first study on the possibility to determine the gluon structure function based on the leading order QCD analysis. We have shown that the gluon structure function $xG(x)$ can be determined by the ATLAS experiment in the range $0.005 < x < 0.04$ for Q^2 values between 440 GeV^2 and $2{\cdot}10^4$ GeV^2 by using the cross section for producting a jet opposite to a direct photon in the LHC pp collisions at $\sqrt{s}$ = 14 TeV. The prompt photon away-side jet cross section is obtained for central photon production where the background from π° and η is not taken into account. The precision on $xG(x)$ is limited by the systematic error of the order of 11.2-21.7 %. The results are in agreement with the theoretical gluon parametrization HMRS B1. The variation between

simulated data and theory is estimated to be less than 5 %, which is due to the fact that the Q^2 dependence of the $xG(x)$ values has been neglected.

As a next step, it is mandatory to extend this study to next-to-leading order QCD. For this purpose, the computer code of ref. [5] which includes the $O(\alpha_s)$ QCD corrections can be used. A procedure has to be implemented to unfold the gluon density from the observed (simulated) distributions, with a (possibly iteration) numerical approach. At an even later stage, the information from direct-photon production has to be combined with other measurements (e.g. $jets$, W, Z) to perform a global fit of parton distributions. One has to take into account background sources for prompt photon production in the analysis to study the influence of the background substraction on the determination of the gluon density.

Acknowledgments

We would like to thank F. Gianotti, J. Collot, S. Tapprogge and S. Frixione for helpful discussions and comments on the manuscript. El M. Ab. is also thankful to S. Tapprogge for useful suggestions during this work.

References

[1] T.Sjöstrand, Computer Physics Commun.82 (1994) 74.

[2] Elzbieta Richter-Was, Daniel Froidevaux and Luc Poggioli, Note interne ATLAS PHYS-98-131 (1998).

[3] J.F.Owens, Large-momentum-transfer Production of Direct Photons, Jets, and Particles, Reviews of Modern Physics 59 (1987) 465.

[4] E.N.Argyres et al., Physical Review D 35 (1987) 1584; S.Ellis, M.Kisslinger, Physical Review D 9 (1974) 2027.

[5] S.Frixione, private communication.

[6] A.Dell'Acqua, D.Froidevaux, T.Hansl-Kozanecka, S.O'Neale, G.Poulard, E.Richter-Was, M.Stavrianakou, Note interne ATLAS PHYS-97-102 (1997).

[7] CTEQ collaboration, MSUHEP-60426, CTEQ-64.

[8] A.D.Martin, R.G.Roberts, W.J.Stirling, Physics Letters 354 B (1995) 155; RAL Preprint, RAL /95-021 (1995).

[9] M.Glück, E.Reya, A.Vogt, Z. Physics C 48 (1990) 471; Z. Physics C 53 (1992) 127; Physics Letters 306 B (1993) 391.

[10] E.Reya, Physics Reports 69 (1981) 195-333.

[11] A.D.Martin, W.J.Stirling, R.G.Roberts, Physical Review D 50 (1994) 6734.

[12] W.J.Marciano, Physical Review D 29 (1984) 580.

[13] H.L.Lai et al, Physical Review D 55 (1997) 1280.

[14] F.James, MINUIT-Reference Manual (Version 94.1), Program Library D506.CERN, 1994.

[15] P.N.Harriman, A.D.Martin, R.G.Roberts, W.J.Stirling, Physical Review D 42 (1990) 798; Physics Letters 243 B (1990) 421.

[16] A.D.Martin, R.G.Roberts, W.J.Stirling, R.S.Thorne, hep-ph/9803445.

[17] A.D.Martin, R.G.Roberts, W.J.Stirling, Physical Review D 47 (1993) 867.

[18] CTEQ Collaboration, hep-ph/9903282.

[19] P.Aurenche, R.Baier, M.Fontannaz, J.F.Owens, M.Werlen, Physical Review D 39 (1989) 3275.

[20] J.Morfin, W.K.Tung, Z. Physics C 52 (1991) 13.

[21] D.W.Duke, J.F.Owens, Physical Review D 30 (1984) 49.

[22] E.A.Kuraev, L.N.Lipatov, V.S.Fadin, Sov.Phys.JETP 45 (1977) 199; Ya.Ya.Balitsky, L.N.Lipatov, Sov.J.Nucl.Phys. 28 (1978) 822.

[23] UA2 collaboration, Physics Letters B 299 (1993) 174-182.